

DTIC FILE COPY

2

AD-A224 122

NAVAL POSTGRADUATE SCHOOL

Monterey, California



THESIS

DTIC
ELECTE
JUL 20 1990
S E D

UNIPOLAR ARCING
ON THE
CATHODE SURFACE
OF A HIGH VOLTAGE DIODE

by

Stephen A. Minnick

December 1989

Thesis Advisor

F. Schwirzke

Approved for public release; distribution is unlimited.

99 07 20 070

Unclassified

SECURITY CLASSIFICATION OF THIS PAGE

REPORT DOCUMENTATION PAGE				
1a REPORT SECURITY CLASSIFICATION Unclassified		1b RESTRICTIVE MARKINGS		
2a SECURITY CLASSIFICATION AUTHORITY		3. DISTRIBUTION/AVAILABILITY OF REPORT Approved for public release; distribution is unlimited		
2b DECLASSIFICATION/DOWNGRADING SCHEDULE				
4. PERFORMING ORGANIZATION REPORT NUMBER(S)		5. MONITORING ORGANIZATION REPORT NUMBER(S)		
6a NAME OF PERFORMING ORGANIZATION Naval Postgraduate School	6b OFFICE SYMBOL (If applicable) 33	7a NAME OF MONITORING ORGANIZATION Naval Postgraduate School		
6c ADDRESS (City, State, and ZIP Code) Monterey, CA. 93943-5000		7b. ADDRESS (City, State, and ZIP Code) Monterey, CA. 93943-5000		
8a NAME OF FUNDING/SPONSORING ORGANIZATION	8b OFFICE SYMBOL (If applicable)	9. PROCUREMENT INSTRUMENT IDENTIFICATION NUMBER		
8c ADDRESS (City, State, and ZIP Code)		10. SOURCE OF FUNDING NUMBERS		
		PROGRAM ELEMENT NO.	PROJECT NO.	TASK NO. WORK UNIT ACCESSION NO.
11 TITLE (Include Security Classification) UNIPOLAR ARCING ON THE CATHODE SURFACE OF A HIGH VOLTAGE DIODE				
12 PERSONAL AUTHOR(S) Stephen A. Minnick				
13a TYPE OF REPORT Master's Thesis	13b TIME COVERED FROM _____ TO _____	14 DATE OF REPORT (Year, Month, Day) December 1989	15 PAGE COUNT 38	
16 SUPPLEMENTARY NOTATION The views expressed in this thesis are those of the author and do not reflect the official policy or position of the Department of Defense or the U. S. Government.				
17 COSATI CODES		18 SUBJECT TERMS (Continue on reverse if necessary and identify by block number)		
FIELD	GROUP	SUB-GROUP		
		Unipolar arcing, laser-surface interaction, whisker explosion,		
19 ABSTRACT (Continue on reverse if necessary and identify by block number)				
<p>The idea of electron emission from an exploding cathode whisker has been reported on many times by various research groups. However, since the reported estimates of current density from the cathode spots vary widely over several orders of magnitude, it is clear that the actual mechanism of explosive emission is not well understood.</p> <p>Plasma surface interaction via unipolar arcing can be shown to be able to supply the necessary current density to initiate explosive emission. Joule heating of the whisker by unipolar arcing is much greater than for either field emitted or space charge limited current flow. It has now been shown experimentally that unipolar arcing occurs not only in a laser induced plasma surface interaction, but also in a vacuum diode discharge at the cathode surface. The unipolar arcing process forms the initial breakdown plasma in each case.</p>				
20 DISTRIBUTION/AVAILABILITY OF ABSTRACT <input checked="" type="checkbox"/> UNCLASSIFIED/UNLIMITED <input type="checkbox"/> SAME AS RPT <input type="checkbox"/> DTIC USERS		21. ABSTRACT SECURITY CLASSIFICATION Unclassified		
22a NAME OF RESPONSIBLE INDIVIDUAL F. Schwirzke		22b TELEPHONE (Include Area Code) (408) 646-2431	22c OFFICE SYMBOL 61Sw	

DD FORM 1473, 84 MAR

83 APR edition may be used until exhausted.
All other editions are obsolete

SECURITY CLASSIFICATION OF THIS PAGE

U.S. Government Printing Office: 1988-606-243

Unclassified

Approved for public release; distribution is unlimited.

Unipolar Arcing
on the
Cathode Surface
of a High Voltage Diode

by

Stephen A. Minnick
Lieutenant, United States Navy
B.S., Pennsylvania State University, 1981

Submitted in partial fulfillment of the
requirements for the degree of

MASTER OF SCIENCE IN PHYSICS

from the


NAVAL POSTGRADUATE SCHOOL
December 1989


Author:


Stephen A. Minnick

Approved By:


F. Schwirzke, Thesis Advisor


K. K. Maruyama, Second Reader


K. E. Woehler, Chairman,
Department of Physics

ABSTRACT

The idea of electron emission from an exploding cathode whisker has been reported on many times by various research groups. However, since the reported estimates of current density from the cathode spots vary widely over several orders of magnitude, it is clear that the actual mechanism of explosive emission is not well understood.

Plasma surface interaction via unipolar arcing can be shown to be able to supply the necessary current density to initiate explosive emission. Joule heating of the whisker by unipolar arcing is much greater than for either field emitted or space charge limited current flow. It has now been shown experimentally that unipolar arcing occurs not only in a laser induced plasma surface interaction, but also in a vacuum diode discharge at the cathode surface. The unipolar arcing process forms the initial breakdown plasma in each case.



iii

Accession For	
NTIS GRA&I	<input checked="" type="checkbox"/>
DTIC TAB	<input type="checkbox"/>
Unannounced	<input type="checkbox"/>
Justification	
By _____	
Distribution/	
Availability Codes	
Dist	Avail and/or Special
A-1	

TABLE OF CONTENTS

I.	INTRODUCTION	1
II.	BACKGROUND	5
	A. ONSET OF SURFACE BREAKDOWN	5
	1. High Voltage Induced Plasma Formation ...	5
	2. Laser Induced Plasma Formation	8
	B. UNIPOLAR ARCING	11
III.	EXPERIMENT	20
IV.	CONCLUSIONS AND RECOMMENDATIONS	27
	LIST OF REFERENCES	30
	INITIAL DISTRIBUTION LIST	31

ACKNOWLEDGEMENT

I would like to thank several people for their help in completing this report. I thank Dr. Fred Schwirzke for his efforts in pushing me to understand the various mathematical descriptions of the physical processes involved. Without his urging, I never would have learned as much as I have about plasma-surface interactions. I also wish to thank Don Snyder and Harold Rietdyk for their help and especially their time in operating the Flash X-Ray machine for my experiments. They were always available when I needed them, which is quite a feat considering their many duties around the school.

Stephen A. Minnick
14 December 1989

I. INTRODUCTION

The concept of electron emission from an exploding cathode spot is well established in the literature [Ref. 1-4]. However, since the estimates of current density j from a cathode spot vary by several orders of magnitude, from 10^5 A/cm² [Ref. 5] to 10^9 A/cm² [Ref. 1], the details of the actual mechanism of explosive emission are not yet fully understood.

A cathode "whisker" represents any electron emitting spot on the surface of a cathode, such as a microprojection, adsorbed contaminant, metal grain boundary, etc, where the electric field and the field emission current are enhanced by one to several orders of magnitude. The breakdown process in a vacuum diode is most commonly considered to be initiated by the field emission of electrons from a cathode whisker due to the externally applied electric field. The resulting field emission current density, given by the Fowler-Nordheim equation [Ref. 1], is assumed to be large enough to cause the whisker to explode due to Joule heating effects. The exploding whisker forms a dense plasma immediately above the

spot which shields the local cathode area from the external field, since the plasma surface then acts as a virtual cathode. The diode current density is then given by the Child-Langmuir law for space charge limited currents. To determine how large a current density is required to explode a cathode whisker by Joule heating, the whisker is assumed to be a cylinder of height L and radius R . The total power dissipated in the whisker is then

$$\Delta Q/\Delta t = iv = j\pi R^2 v \quad (1)$$

where ΔQ is the energy deposited, i is the whisker current, j is the current density, and v is the whisker potential drop. With the electric field of the whisker $E = j/\sigma = v/L$, $v = jL/\sigma$ and the volume $V = \pi R^2 L$,

$$\Delta Q/\text{atom} = j^2 V \Delta t / n \sigma V \quad (2)$$

where σ is the material conductivity and n is the atomic density. For stainless steel, $\sigma = 1.4 \times 10^5 / (\Omega\text{-cm})$ and $n = 8.2 \times 10^{22} \text{ cm}^{-3}$. This leads to an energy per atom of

$$\text{eV/atom} = 5.4 \times 10^{-10} j^2 \Delta t \quad (3)$$

where j is in A/cm^2 and Δt is in seconds. In order to explode the bulk whisker into the plasma state, an energy on the order of 5.4 eV/atom must be deposited. This is roughly the energy necessary to break the metallic bonds of the stainless steel, vaporize, and then ionize the atoms of the whisker. The current density j required to deposit this energy in the time frame of a few nanoseconds (the observed length of time for breakdown to occur) per equation (3) is greater than 10^9 A/cm^2 . However, calculations show that the space charge limited current density for a typical diode voltage of 1 MV with a cathode-to-anode spacing of $d = 2.54 \text{ cm}$ (assuming a uniform electric field) is $j_{\text{CL}} = 3.6 \times 10^2 \text{ A/cm}^2$. This is many orders of magnitude smaller than the necessary current density j for bulk whisker explosion found above.

The variation of a typical diode current with time is shown in Figure 1. The process of transition from field emitted current density j_{FE} with electric field at the cathode surface being of maximum value $E = E_{\text{FE}} = E_{\text{max}}$, to space charge limited current density j_{CL} with $E = E_{\text{CL}} \approx 0$ is still unknown. Also unknown is the mechanism by which the large current density for explosion is generated.

This report will describe how the transition from j_{FE} to j_{CL} can occur by the mechanism of unipolar arcing (UPA). It

will also show how UPA can supply the necessary current density for cathode spot explosion in a nanosecond time frame even though the actual diode gap current is space charge limited at a much lower value. Lastly, this report will describe experiments performed showing that unipolar arcing does indeed take place on the cathode surface of a vacuum diode.

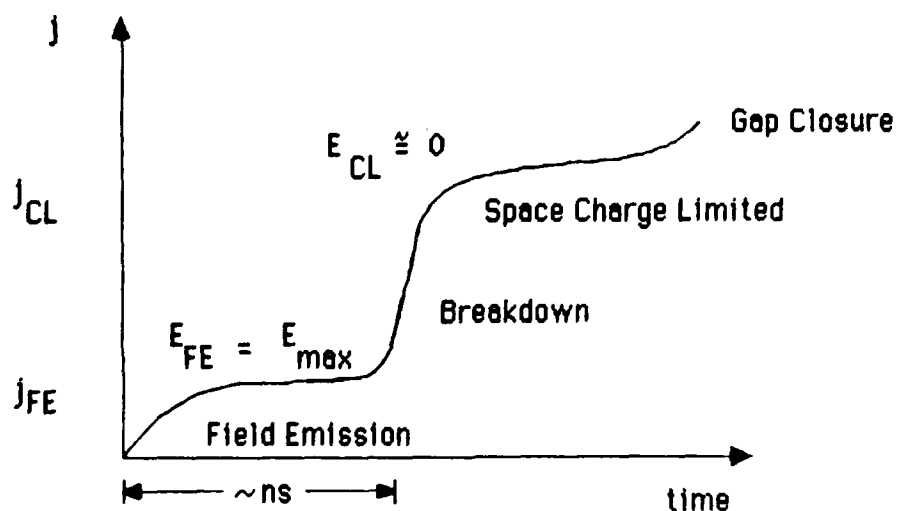


Figure 1: Variation of typical diode gap current with time. j_{CL} is the Child-Langmuir space charge limited current density. j_{FE} is the field emitted current density. The electric fields shown are the electric fields at or very near the cathode surface corresponding to the curve plateaus. Gap closure defines the point at which the breakdown arc extends across the diode gap.

II. BACKGROUND

A. ONSET OF SURFACE BREAKDOWN

1. High Voltage Induced Plasma Formation

Adsorbed neutral contaminants, such as O_2 , H_2 , and other gases are always present on the surfaces of electrodes in a vacuum diode. These contaminants, as well as whiskers on the cathode surface, provide spots for enhanced field emission of electrons in a high ($> 10^5$ V/cm) electric field. Desorption and ionization of the contaminants from the area of the cathode spots occurs due to the field emitted electrons. The combined effects of the electric field, the emitted electrons, and the subsequent ion bombardment of the cathode spots continue to stimulate desorption [Ref. 6].

Assuming one contaminant monolayer of 2×10^{15} atoms/cm² is suddenly released from the surface with a room temperature sound velocity $v = 3.3 \times 10^4$ cm/s, a dense neutral gas layer is formed. Taking $t = 3$ ns as the average time span of release of the monolayer [Ref. 1], the average density of the neutral gas is $n_0 = (2 \times 10^{15} \text{ atoms/cm}^2)/vt = 2 \times 10^{19}/\text{cm}^3$ (almost atmospheric density). The mean free path for ionizing a neutral

atom is $\ell = 1/n_0\sigma_0$, which depends on the cross section for ionization σ_0 , which in turn depends on the electron energy. A field emitted electron gains an energy of 100 eV in a distance $vt = 10^{-4}$ cm in an electric field of 10^6 V/cm. For neutral contaminants (such as O_2 , H_2 , and other gases), σ_0 has a maximum value of approximately 10^{-16} cm² for 100 eV electrons. Therefore, $\ell = 5 \times 10^{-4}$ cm and thus $(vt/\ell) \times 100\% = 20\%$ of the emitted electrons can possibly collide with neutrals within $vt = 10^{-4}$ cm. The onset of surface breakdown in a diode is delayed on the order of a few nanoseconds [Ref. 2] which corresponds to the time of flight of the neutrals to the zone of maximum ionization (where the electrons have gained about 100 eV). [Ref. 7]

The ions formed by this process represent a buildup of positive space charge above the cathode spot which enhances the local electric field E . The field emitted current density j_{FE} increases thereby further increasing neutral atom desorption and subsequently the ionization rate. Additionally, ion bombardment of the local surface area increases releasing more recombination energy which results in the further release of contaminant layers. The increasing positive space charge above the spot implies a higher electric field and therefore the zone of maximum ionization moves closer to the surface.

This in turn causes an even higher ionization rate since the neutral density is greater nearer the surface. A double layer forms between the electrons moving towards the anode and the ions moving towards the cathode. The resultant electric field of the double layer shields the cathode from the diode electric field, and the current density between the plasma and the anode becomes the space charge limited j_{CL} . However, a positive space charge sheath forms where the plasma is in contact with the cathode surface with characteristic width λ_d given by

$$\lambda_d = (\epsilon_0 e V_s / n_e e^2)^{1/2} \quad (4)$$

where V_s is the plasma potential with respect to the cathode. The sheath electric field $E_s = V_s / \lambda_d$ controls the electron emission rate from the cathode spots.

Estimates of the ion and electron density at which a plasma has formed can be made using several criteria. The first is met when the electron density n_e reaches the level as defined by setting the Child-Langmuir law current density j_{CL} equal to $en_e v_e$. This implies that the local electric field E is approximately zero and therefore the external field is screened from the cathode surface by the plasma. Taking

10 eV as a conservative estimate of plasma electron temperature, $v_e = \{2e(10\text{eV})/m_e\}^{1/2} = 2 \times 10^8 \text{ cm/s}$. Therefore, with $j_{CL} = 3.6 \times 10^2 \text{ A/cm}^2$, n_e is approximately $10^{13}/\text{cm}^3$. Alternatively, the second criterion is met when n_e reaches the value as defined by equating the distance travelled by the electrons vt with λ_D , the Debye length. With $vt = 10^{-4} \text{ cm}$ and assuming the same electron temperature as before, n_e is approximately $6 \times 10^{14}/\text{cm}^3$. Either criterion yields an electron density that agrees within a factor of sixty with the other.

2. Laser Induced Plasma Formation

In a laser-surface interaction, the initial energy deposition from the laser pulse rather than the field emission of electrons causes desorption of a layer of neutral contaminants. Since there is no external electric field to cause electron emission, the process by which ionization of the released neutrals occurs can not be the same as in the case of the high voltage induced plasma formation. While it is known that a $1.06 \text{ } \mu\text{m}$ Neodymium laser does induce plasma formation at the surface of a metal target [Ref. 8], the actual process of ionization by this laser radiation is still unknown. Photoionization of the neutrals cannot occur since the laser photon energy is insufficient for excitation. It is usually assumed that "stray" electrons present in the

neutral cloud initiate ionization, and the resultant secondary electrons continue the process. However, observation of arcing damage on the surfaces of laser irradiated metal targets [Ref. 8] show a pattern of interference rings with greater arc densities where the laser intensity was largest. If "stray" electrons, which should be randomly distributed in the neutral cloud, were responsible for the initiation of ionization, the arcing damage would be more uniform across the surface. Since experimental evidence exists showing that this is not the case, ionization must be initiated by some process of laser induced emission of electrons from the surface.

One speculation for the ionization process is that the necessary electron emission is caused by laser "field" emission. The electromagnetic radiation incident on the target surface sets up a standing wave electric field distribution. The peak field occurs at $\lambda/4 = 0.26 \mu\text{m}$. The dimensions of surface inhomogeneities and contaminants, hereafter defined as "spots", could easily be of this order meaning that the maximum electric field intensity occurs at the tips of the spots. With the onset of laser induced microarcing occurring at an average surface energy density $S_a = 5.4 \text{ MW/cm}^2$ [Ref. 8] and with $S_a = 4E_0^2/\eta_0$, where η_0 is the

impedance of free space, the peak electric field E_0 is approximately 2×10^4 V/cm. This is within an order of magnitude of the necessary minimum field strength of 10^5 V/cm [Ref. 6] required for the initiation of electron field emission. The nonuniformity of the laser output would generate the observed ring patterns on the metal surface due to the variations in local surface energy density above and below the 5.4 MW/cm^2 threshold.

The buildup of positive space charge above the electron emitting spot forms a potential resulting in an electric field between the ion cloud and the surface. This field accelerates ions to the surface resulting in increased energy deposition and subsequent neutral desorption. The positive space charge sheath of the plasma cloud in contact with the surface has a width given by the Debye length

$$\lambda_D = (\epsilon_0 K T_e / n_e e^2)^{1/2} \quad (5)$$

and an electric field $E_s = V_f / \lambda_D$, where V_f is the cloud floating potential. The result of the continued production of ions and electrons above the spot is that the surface is eventually screened from direct laser radiation impingement when the cloud density reaches the critical density as defined

by the plasma frequency $\omega_p = (n_e e^2 / \epsilon_0 m_e)^{1/2}$. Energy transport to the cathode surface then occurs due to heat conduction by electrons and short wavelength plasma radiation [Ref. 8] which stimulates additional contaminant desorption, ionization and subsequent plasma formation.

B. UNIPOLAR ARCING

As described by Schwirzke in Reference 8, the unipolar arc (UPA) is the primary plasma surface interaction process. The continued emission and ionization of neutral contaminants and metal atoms creates a small dense plasma jet above the area of the spot which increases the local plasma pressure p_e and hence results in an ambipolar electric field $E_{amb} = -\nabla p_e / en_e$ in the radial direction tangential to the cathode surface. This field reduces the plasma sheath potential in a ring-like area around the cathode spot which enables more electrons from the high energy tail of the Maxwellian distribution to reach the cathode surface. The amount of sheath reduction is found by integrating the radial electric field distribution resulting in

$$\Delta V(r) = [KT_e / e] \ln[n_e(r) / n_{e0}] \quad (6)$$

where $n_e(r)$ is the plasma electron density in the radial direction around the cathode spot and n_{e0} is the bulk plasma electron density. A plot of this potential (Figure 2) shows that for $r > r_f$, $V_s < V_f$, where V_s is the local plasma jet sheath potential and V_f is the floating potential at r_f , where the ion and electron current flows through the sheath to the surface are equal. For $r > r_f$, more electrons can return to the cathode surface completing the current loop of the unipolar arc. A schematic of the unipolar arc model is shown in Figure 3.

The loss of these high energy electrons to the surface decreases the potential difference ΔV , defined as $V_f - V_s$, to which the electrons are exposed. This results in a reduced radial electric field E_r which allows more high energy electrons from the plasma cloud to escape since

$$E_r(r) = -\Delta V / \Delta r < E_{amb} . \quad (7)$$

The resulting fields and current flows are as shown schematically in Figure 4.

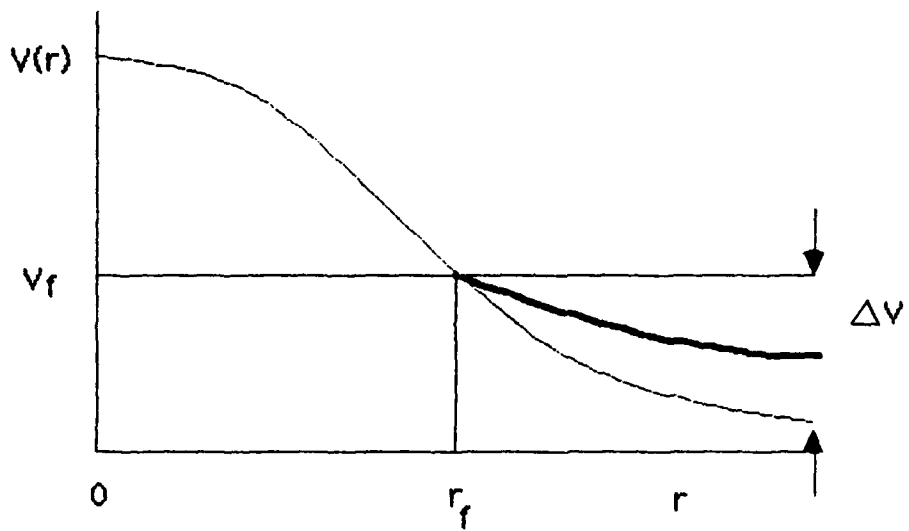


Figure 2: Plot of plasma sheath potential as a function of radial plasma dimension. Light curve is without electron losses to the surface. Heavy curve is with electron losses. The electron emitting cathode spot is at $r = 0$.

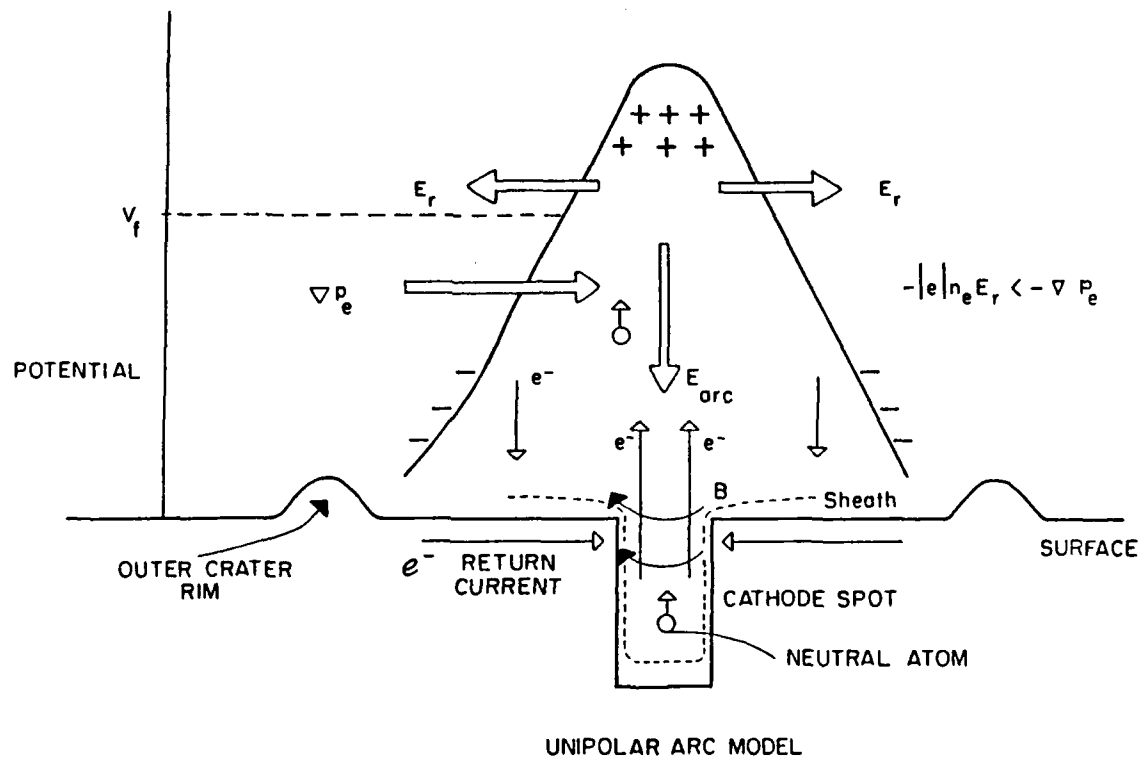


Figure 3: Schematic of the unipolar arc model for a vacuum diode.

The equation of motion for the electron fluid is given by

$$-enE - \nabla p + enj/\sigma = 0 \quad (8)$$

where j is the current density, σ is the electrical conductivity, $B = 0$, and the electron inertial term is assumed insignificant over the time scale of the arc. If $E = E_{amb}$, then $j = 0$ and there is no net current in the plasma. If, however, $E = E_r$, then

$$-enE_r - \nabla p = -enE_{amb} \quad (9)$$

which is equivalent to a net force F_{net} acting on the electrons and pointing radially out of the plasma. This is the driving force of the unipolar arc. For convenience, a new effective electric field E_p is defined as follows

$$-enE_r - \nabla p = -enE_p = F_{net} \quad (10)$$

which results in an electron equation of motion of

$$-enE_p = -enj/\sigma \quad (11)$$

Figure 5 shows the electron density profile with the effective field and net force superimposed. It follows that as more electrons escape from the plasma to the surface, ΔV is decreased and therefore E_p is increased resulting in an increase in j . This leads to the escape of even more electrons resulting in a positive feedback mechanism. j continues to increase which results in an extremely rapid rise in cathode whisker temperature due to Joule heating. This is the mechanism by which a whisker explosion can occur even though the predicted Child-Langmuir space charge limited current and the field emitted current are insufficient to cause the necessary whisker heating. The chain of events leading to whisker explosion are summarized in Figures 6.1 - 6.3.

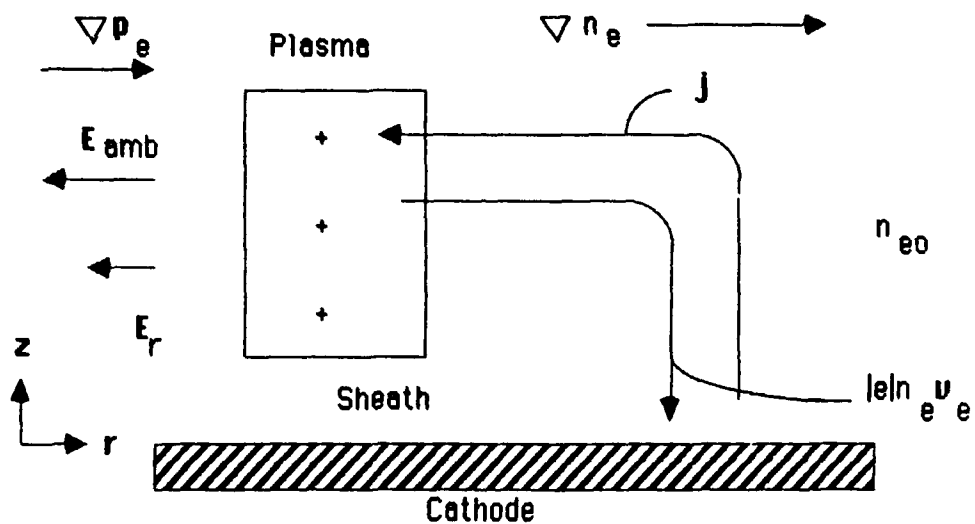


Figure 4: Representative plot of unipolar arc fields and current flows. The paths shown for the electrons flowing towards the cathode surface and for the current density to the plasma are intended as an illustration and are not meant to represent individual electron paths or actual current flow.

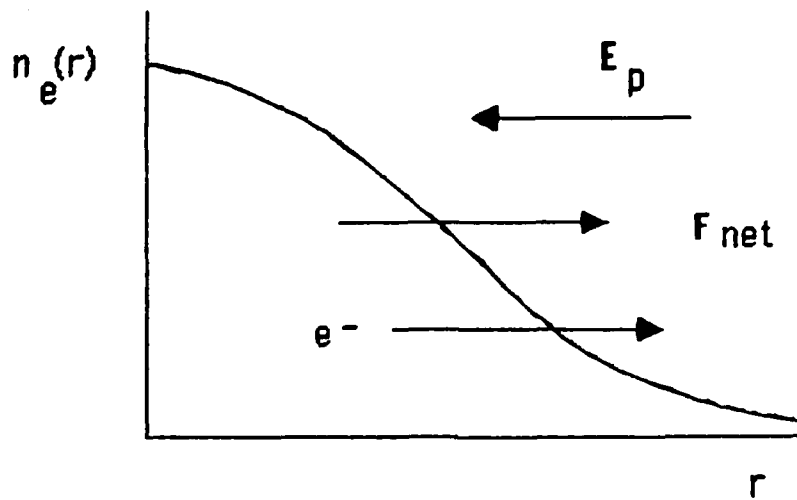
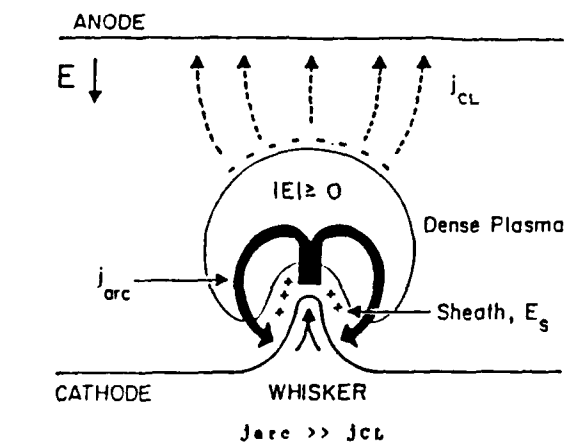
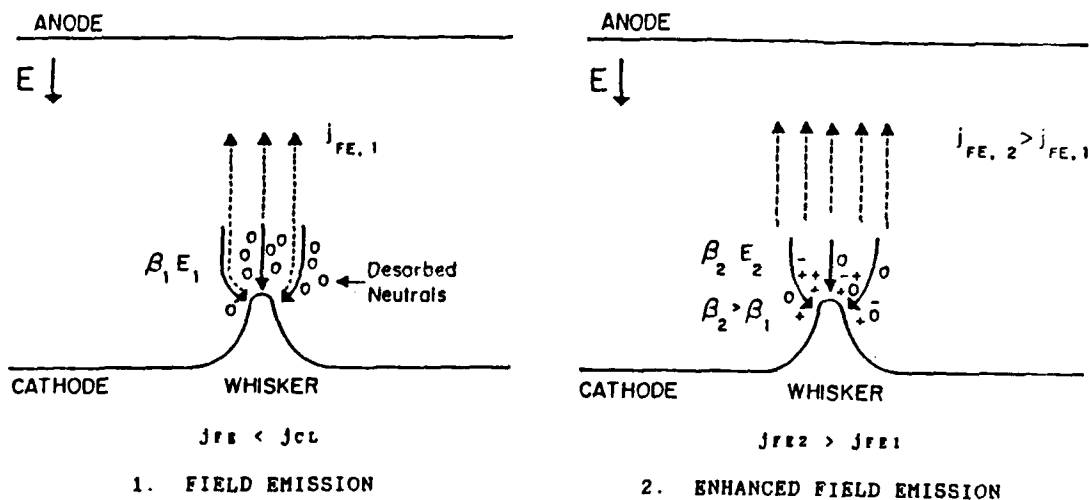


Figure 5: Plot of plasma electron density showing the effective field E_p and the net force on the electrons due to E_p .



3. WHISKER EXPLOSION BY UNIPOLAR ARCING

The dense plasma shields the cathode from the externally applied field E .

- j_{FE} = Electron Field Emission Current Density
- j_{CL} = Electron Child-Langmuir Space Charge Limited Current Density
- β = Electric Field Enhancement Factor
- E_s = Sheath Electric Field

Figure 6: Sequence of events leading to whisker explosion by unipolar arcing.

III. EXPERIMENT

In order to determine whether the vacuum diode breakdown mechanism is cathode spot explosion via unipolar arcing, five breakdown events were performed using a Model 112A Pulserad Pulsed X-Ray Generator [Ref. 9]. The cathode was a stainless steel cylindrical rod with a diameter of 3.18 cm. The cathode was repolished metallographically using a fine slurry of 0.05 μm Al_2O_3 after each event. The diode voltage and cathode-to-anode spacing were varied as in Table 1 in order to observe the effects of different parameters on the possibility of unipolar arc formation. As it turned out, characteristic unipolar arcing craters were observed on all five exposed cathodes. However, as expected, the higher voltage shots displayed a greater density of craters and a higher degree of cathode surface melting than did the lower voltage shots.

Figure 7a shows a close-up of unipolar arc craters on cathode surface number 3 after a 20 ns FWHM duration shot. For comparison, Figure 7b is a close-up of laser induced unipolar arcs on the surface of a stainless steel target taken after one shot from a Neodymium laser of 25 ns FWHM and

5.4 MW/cm². Figure 8a shows cathode surface number 2 after a similar shot at a higher voltage, while Figure 8b shows the burn pattern on a target from a laser shot. Figures 9a and 9b show respectively the areas near the edges of heavily damaged sections on cathode number 3 and on a target exposed to unfocused laser radiation.

Cathode surfaces numbers one and two were exposed to the greatest diode potential difference (1.1 MV) and exhibited the most extensive cratering. The exposed areas were 100% cratered with many craters overlapping and severe surface melting in evidence (Figure 8a). Cathode surfaces numbers three and four were exposed to the lowest potential difference (0.7 MV) and exhibited the least cratering with numerous individual craters visible (Figure 7a). As can be seen in Figure 10, approximately 15% of these cathode surfaces were cratered with surface melting evident only in the most heavily damaged area. The dramatic increase in the total area of cathode surface damage with less than a doubling of applied electric field strength implies that there may be a possible threshold field value at which damage begins to increase rapidly. Further investigation may yield such a value.

The similarity of the crater patterns on all of these surfaces leads to the conclusion that the cathode spots in each case were formed by the unipolar arcing process, and that plasma formation by this process leads to vacuum breakdown.

TABLE 1: PARAMETERS OF THE FIVE DIODE BREAKDOWN EVENTS

SHOT NUMBER	DIODE VOLTAGE ¹ (MV)	GAP SPACING (cm)	ELECTRIC FIELD (10 ⁵ V/cm)	DIODE CURRENT ¹ (kA)
1	1.1	1.91	5.8	21
2	1.1	2.54	4.3	21
3	0.70	1.91	3.7	14
4	0.70	2.38	2.9	14
5	0.84	2.54	3.3	17

¹ The values for diode voltage and current were taken from Reference 9 and were not measured during the experiments.



Figure 7a: Closeup of diode induced unipolar arc craters on cathode surface number 3.



Figure 7b: Closeup of laser induced unipolar arc craters on a stainless steel target.

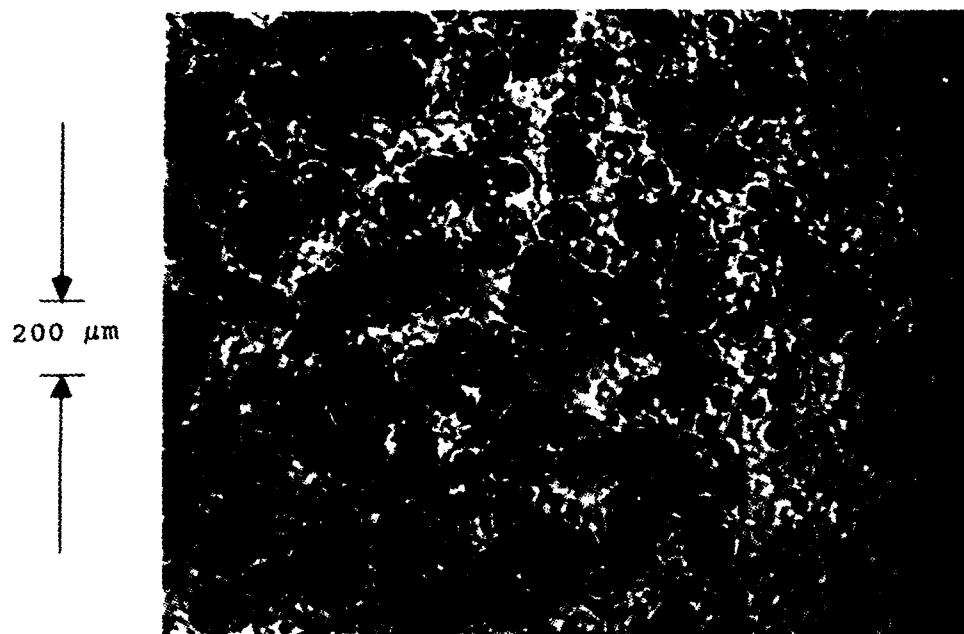


Figure 8a: Diode induced unipolar arc craters on cathode surface number 2.



Figure 8b: Laser induced unipolar arc craters on a stainless steel target.

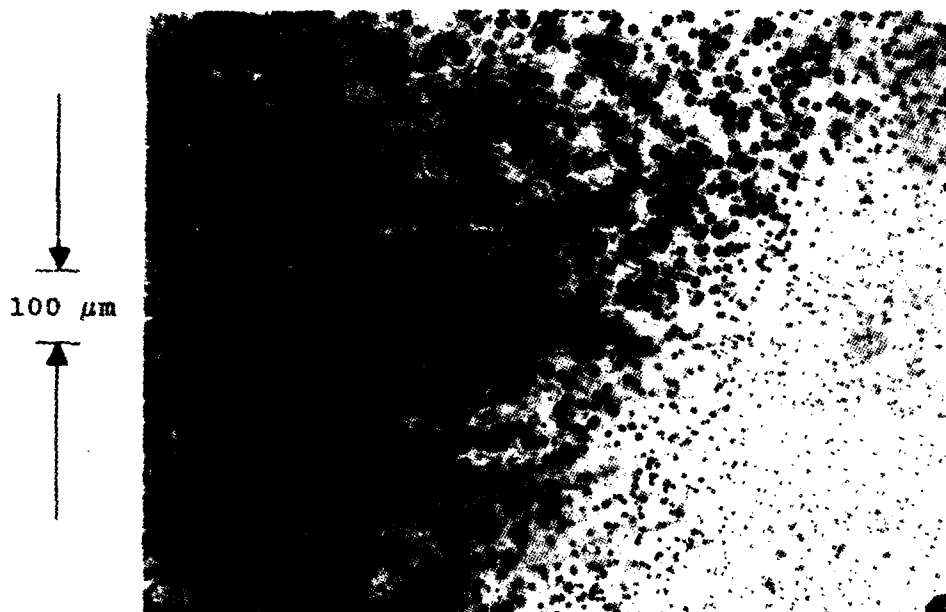


Figure 9a: Area near an edge of a heavily damaged section of cathode number 3 showing the spatial variation in unipolar arc crater density.



Figure 9b: Area near an edge of an unfocused laser damaged section of metal target showing the spatial variation in unipolar arc crater density.

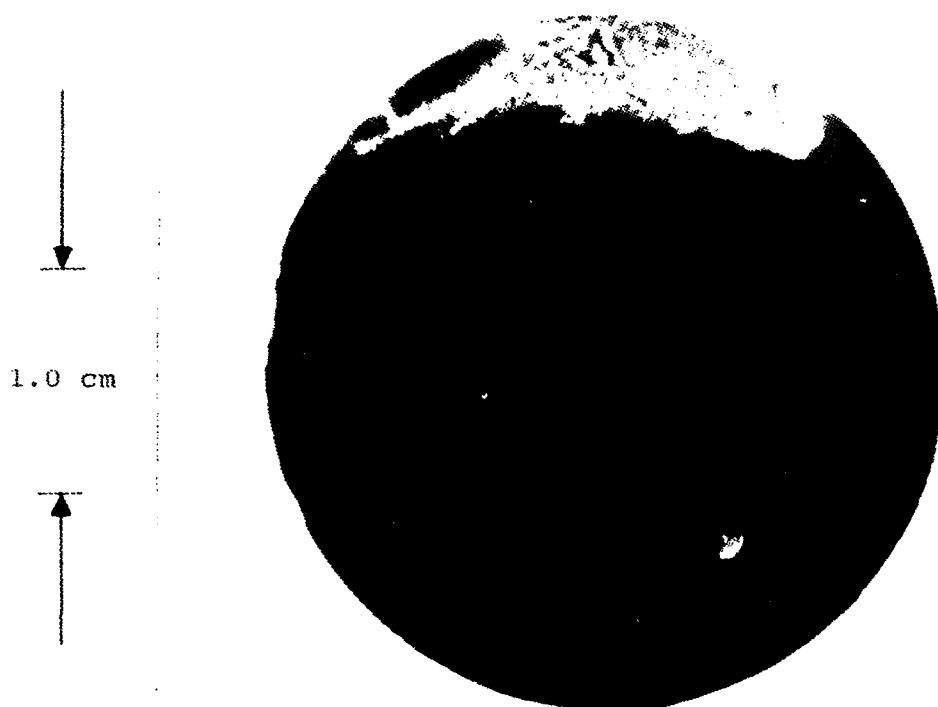


Figure 10: Photograph of cathode surface number three. The dark area is the undamaged polished metal. The light areas are the sections of surface that underwent arcing. Overlapping unipolar arc craters are visible in the heavily damaged area. Individual craters (not visible) appear in the fringes of the light areas at the limit of the plasma cloud expansion.

IV. CONCLUSIONS AND RECOMMENDATIONS

This report has described how the mechanism of unipolar arcing can supply the necessary current density for explosive plasma formation and electron emission from a cathode surface spot in a nanosecond time frame. In addition, it has been shown that this mechanism does indeed occur on the surface of a vacuum diode cathode with an externally applied electric field, and that it is remarkably similar to the interaction between a laser produced plasma and a metal target surface with no external field. The following conclusions are also made:

- Surface breakdown is initiated by the ionization of desorbed contaminants, mostly gases, by field emitted electrons. Since this requires energy deposition only within a few contaminant monolayers at a time instead of an entire whisker volume, and since the neutral contaminants are only loosely bound to the surface by relatively weak Van der Waal forces, the onset of surface breakdown by this mechanism requires much less current and energy than vaporization and ionization of the entire cathode whisker.

- The driving force behind the unipolar arc is the pressure and electric field distributions resulting from the highly localized increase of plasma density above the electron emitting cathode spot.

- The closure of the diode gap results from the expansion of the plasma ions under the influence of the plasma pressure gradient. This can occur since the external electric field is effectively screened from the dense plasma when the current to the anode becomes space charge limited. The ions thus see no retarding external field.

- Since the external field is screened from the cathode surface, the whisker current is no longer determined by the space charge limited current. Hence the unipolar arc current density can be many orders of magnitude greater than the Child-Langmuir space charge limited diode current density.

- The large variation in published values for cathode spot current densities can be explained by the fact that the unipolar arc current has not been measured in determinations of the overall diode current density.

The following areas are recommended for additional research:

- Study of surface conditions that can enhance/reduce breakdown such as contaminants, gas release rates, surface

roughness, etc.

- Determination of methods to prevent unipolar arc damage.

- Study of effects of unipolar arcing on anode surface plasma interactions.

- Determination of the process of breakdown and plasma formation at the anode surface and its effects (if any) on cathode surface breakdown processes.

- Determination of a possible threshold external electric field strength at which the amount of cathode surface damage increases suddenly.

- Study of the possible occurrence of unipolar arcing in the waveguides of high power microwave devices.

LIST OF REFERENCES

1. Litvinov, E.A., and others, "Field Emission and Explosive Electron Emission Processes in Vacuum Discharges," Sov. Phys. Usp., v. 26(2), pp 138-159, 1983.
2. Lyubimov, G.A., and others, "The Cathode Spot of a Vacuum Arc," Sov. Phys. Usp., v. 21(8), pp 693-718, 1978.
3. Fursey, G.N., "Electrical Breakdown in Vacuum," IEEE Transactions on Electrical Insulation, EI-20 No.5, pp 659-841, 1985.
4. Rakhovsky, V.I., IEEE Transactions on Plasma Science, PS-15, pg 481, 1987.
5. Rakhovsky, V.I., IEEE Transactions on Plasma Science, PS-12, pg 199, 1984.
6. Halbritter, J., "Dynamical Enhanced Electron Emission and Discharges at Contaminated Surfaces," Appl. Phys., v. 39, pg 49, 1986.
7. Schwirzke, F., "Laser Induced Breakdown and High Voltage Induced Breakdown on Metal Surfaces," 1989.
8. Schwirzke, F., "Laser Induced Unipolar Arcing," Laser Interaction and Related Phenomena, v. 6, pp 335-351, Plenum Publishing Corporation, 1984.
9. Physics International Company, Model 112A Pulserad Pulsed X-Ray Generator Operations and Maintenance Manual, January 1986.

INITIAL DISTRIBUTION LIST

	No. Copies
1. Defense Technical Information Center Cameron Station Alexandria, Virginia 22304-6145	2
2. Library, Code 0142 Naval Postgraduate School Monterey, California 93943-5002	2
3. Dr. K. E. Woehler, Code 61Wh Department of Physics Naval Postgraduate School Monterey, California 93943-5100	1
4. Dr. F. Schwirzke, Code 61Sw Naval Postgraduate School Monterey, California 93943-5100	5
5. Dr. X. K. Maruyama, Code 61Mx Naval Postgraduate School Monterey, California 93943-5100	2
6. Physics Library, Code 61 Department of Physics Naval Postgraduate School Monterey, California 93943-5100	2
7. LT Stephen A. Minnick, USN 6 Farmview Street Fairchance, Pennsylvania 15436	2
8. Mr. Donald Snyder, Code 61 Accelerator Laboratory Department of Physics Naval Postgraduate School Monterey, California 93943-5100	2